Mycology

An International Journal on Fungal Biology

ISSN: 2150-1203 (Print) 2150-1211 (Online) Journal homepage: www.tandfonline.com/journals/tmyc20

Novel mycelium-based composites with enhanced physico-mechanical properties, as sustainable alternatives for packaging applications

Chathura Madusanka , Dhanushka Udayanga , Renuka Nilmini , Suranga Rajapaksha , Choolaka Hewawasam , Dimuthu Manamgoda , Indunil S. Herath , Mapa Mudiyanselage Sumudu Tharangani Mapa & Juliana Vasco-Correa

To cite this article: Chathura Madusanka , Dhanushka Udayanga , Renuka Nilmini , Suranga Rajapaksha , Choolaka Hewawasam , Dimuthu Manamgoda , Indunil S. Herath , Mapa Mudiyanselage Sumudu Tharangani Mapa & Juliana Vasco-Correa (17 Jul 2026): Novel mycelium-based composites with enhanced physico-mechanical properties, as sustainable alternatives for packaging applications, Mycology, DOI: 10.1080/21501203.2026.2697582

To link to this article: https://doi.org/10.1080/21501203.2026.2697582

Published online: 17 Jul 2026.

MYCOLOGY
https://doi.org/10.1080/21501203.2026.2697582

Taylor & Francis by informa

RESEARCH ARTICLE

OPEN ACCESS Check for updates

Novel mycelium-based composites with enhanced physico-mechanical properties, as sustainable alternatives for packaging applications

Chathura Madusanka[a], Dhanushka Udayanga[b], Renuka Nilmini[c], Suranga Rajapaksha[c], Choolaka Hewawasam[d], Dimuthu Manamgoda[e], Indunil S. Herath[d], Mapa Mudiyanselage Sumudu Tharangani Mapa[a] and Juliana Vasco-Correa[f]

[a]Department of Biosystems Technology, Faculty of Technology, University of Sri Jayewardenepura, Homagama, Sri Lanka; [b]Department of Applied Sciences, Faculty of Humanities and Sciences, Sri Lanka Institute of Information Technology, Malabe, Sri Lanka; [c]Department of Material and Mechanical Technology, Faculty of Technology, University of Sri Jayewardenepura, Homagama, Sri Lanka; [d]Department of Civil and Environmental Technology, Faculty of Technology, University of Sri Jayewardenepura, Homagama, Sri Lanka; [e]Department of Botany, Faculty of Applied Sciences, University of Sri Jayewardenepura, Nugegoda, Sri Lanka; [f]Department of Agricultural and Biological Engineering, Penn State University, University Park, TX, USA

ABSTRACT

Mycelium-based composites (MBCs) are produced through a combination of fungi and lignocellulosic materials. Identifying novel combinations of fungi and lignocellulosic waste is crucial for exploring new material properties. In this study, MBCs were prepared with strains of *Ganoderma orbiforme* and *Lentinus squarrosulus* from Sri Lanka, using three different types of locally sourced lignocellulosic substrates, including *Cocos nucifera* sawdust, *Mangifera indica* sawdust, and coir pith derived from coconut husk. Mycelium inoculum grown on rice seeds was introduced to organic substrates and incubated at 28 °C for 30 d. The resulting composites were separated from the container, dried at 80 °C, and characterised for physicochemical, and microscopic properties. Results indicated that the produced MBCs exhibit properties equivalent to or superior to those of expanded polystyrene (EPS). The Ashby chart generated revealed that MBCs possess properties comparable to cork and other low-density foams, making them suitable for insulating, cushioning, and packaging applications. Among the combinations tested, MBCs made with coir pith and coconut sawdust proved to be the most effective, eco-friendly alternatives to protective packaging.

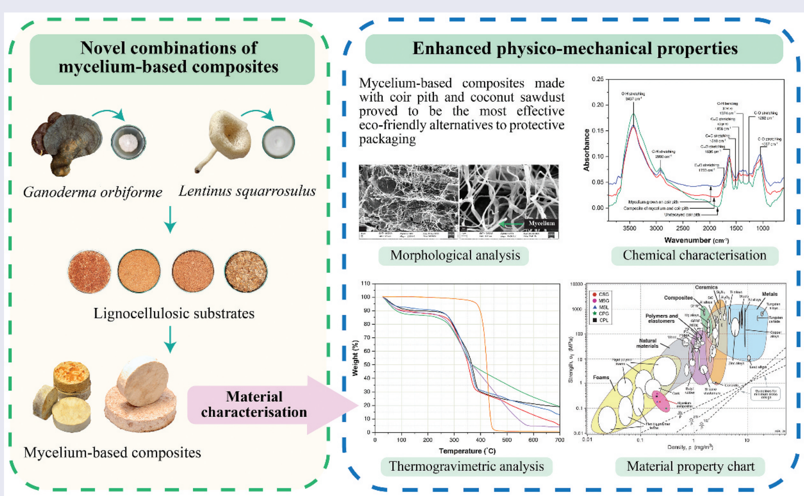

ARTICLE HISTORY
Received 10 September 2025
Accepted 24 May 2026

KEYWORDS
Biocomposites; fungal mycelium; protective packaging material; scanning electron microscopy; styrofoam alternative

CONTACT Dhanushka Udayanga dhanushka.u@sliit.lk Department of Applied Sciences, Faculty of Humanities and Sciences, Sri Lanka Institute of Information Technology, SLIIT Malabe Campus, New Kandy Road, Malabe 10115, Sri Lanka

Published online 17 Jul 2026

1. Introduction

Mycelium-based composites are emerging globally as alternatives to synthetic materials, due to their eco-friendly nature (Alaux et al. 2024; Saini et al. 2024; Majib et al. 2025). Synthetic polymers have a significant environmental impact because they accumulate in large quantities in both inland and aquatic environments. They also release harmful fumes when burned (Majib et al. 2025). The wide-spread use of synthetic foam-based packaging materials, such as expanded polystyrene (EPS), has significantly increased land and water pollution. This is because most commonly used synthetic plastics are not easily compostable (Bhardwaj et al. 2020). Burning expanded polystyrene (EPS) releases hazardous chemicals, including styrene, polycyclic aromatic hydrocarbons (PAHs), carbon black, and carbon monoxide, into the air (Alemu et al. 2022). Additionally, discarded EPS clogs drains, streams, and rivers in large cities and suburban areas, causing widespread environmental issues (Bravo and Hotchkiss 1993; Rossi et al. 2001; Alemu et al. 2022).

Over the past decade, innovative biomimetic processes have gained remarkable attention utilising fungal mycelium to transform lignocellulosic materials into high-value products, such as foams, panels, thin sheets, and leather alternatives (Vaitkus et al. 2022; Dhiman et al. 2024; Kohphaisansombat et al. 2024; Madusanka et al. 2024a).

Mycelium is the vegetative component of filamentous fungi, comprising a network of fine white filaments with diverse layers of protein, glucans, mannans, and chitin (Shin et al. 2025). Fungal mycelium has become a subject of increased interest in research and commercial applications due to its versatility and minimal energy consumption during production (Bhardwaj et al. 2020; Huang et al. 2024). Mycelium can inherently adhere to nearby organic substrates, including sawdust, coffee husk, straw, and bagasse, forming a dense network of filaments (Shin et al. 2025).

Recent studies have revealed the significant potential of mycelium-based composites (MBCs) as alternatives to traditional materials. These materials can be used in packaging, construction, furniture and design, biodegradable mulch, and automotive components (Bhardwaj et al. 2020; Robertson 2020; Alaux et al. 2024). Despite these advancements, significant research gaps persist in the development of MBCs, particularly in optimising fungal species and substrate combinations for specific applications (Sreerag et al. 2025). Selecting appropriate fungal species remains a critical challenge. Factors such as growth rate, mycelium density, cultivation ease, noxiousness, cost of growth media, and structural properties must be balanced (Bhardwaj et al. 2020; Madusanka et al. 2024a).

The characteristics of mycelium-based materials are influenced by various factors, including the substrate used, the fungi strain, the provided environmental conditions in which it grows, and post-processing techniques (Appels et al. 2019; Robertson 2020). Attias et al. (2019) reported that mycelium-based composites can possess properties comparable to EPS and other foams. Biocomposites designed for protective packaging applications must satisfy a combination of key functional properties, including low density for lightweight handling, adequate compressive strength to withstand stacking and impact loads, and low compression set, to recover after deformation. In addition, moisture resistance is also important to maintain structural integrity under humid conditions, while thermal stability and flame retardancy contribute to safety during storage and transport (Madusanka et al. 2024b).

This study aims to discover novel combinations of selected locally sourced lignocellulose substrates and isolates of mushroom-forming fungi belonging to the genera *Ganoderma* and *Lentinus* to produce mycelium-based composites and to fully characterise them for their mechanical and physicochemical properties, assessing their applicability for packaging and other uses.

2. Materials and methods

2.1. Fungal sample acquisition

The fruiting bodies of mushroom-forming fungi were collected from two selected locations in the Western and Southern provinces in Sri Lanka [CM17 from Morawaka, Kodikaragoda (6.273003, 80.484362), M34 from Kottawa, Malapalla (6.846508, 79.981629)]. Small pieces of the mushroom fruiting bodies were surface-sterilised using 70% ethanol, then aseptically transferred onto potato dextrose agar (PDA) plates to isolate fungal cultures. Plates were inoculated at 27 ± 2 °C until mycelial growth was seen. Pure cultures were acquired via successive subculturing and deposited at the University of Sri Jayewardenepura Culture Collection (USJCC) (M34 = USJCC 0191, CM17 = USJCC 0192).

2.2. Molecular identification of fungi

The modified method described by Arnold and Lutzoni (2007) was used to extract genomic DNA from 7-day-old mycelia. The internal transcribed spacer (ITS) region was amplified by PCR utilising the ITS1 and ITS4 primers in a BIORAD® T100TM thermal cycler. The PCR conditions were followed as specified by Manamgoda et al. (2012). The PCR-amplified products were visualised for successful amplification by electrophoresis on a 2% agarose gel, followed by sequencing at the Sanger DNA sequencing centre at Macrogen, Seoul, South Korea. The ITS sequences generated in this study were initially identified with the Basic Local Alignment Search Tool (BLAST) search against the National Center for Biotechnology Information (NCBI) database (www.ncbi.nlm.nih.gov). Sequences exhibiting a similarity of 99% or greater with either ex-type sequences or reliable references were classified as conspecific with the support of morphological and ecological characters of the mushrooms.

2.3. Preparation of grain spawn

Grain spawns were prepared using rice grains in polypropylene bags as described by Madusanka et al. (2024b). The grains were sieved to clean any debris and were then soaked overnight in clean water. These soaked and washed grains were boiled for 15 min. The boiled grains were spread on paper towels to remove excess water and allowed to cool to around 25–30 °C. Then, the grains were mixed with 5% wheat flour, 1.2% commercial-grade gypsum ($CaSO_4$), and 0.3% calcium carbonate ($CaCO_3$) and filled into the polypropylene bags. The bags were subjected to sterilisation in an autoclave at 121 °C and 15 psi for 20 min. For inoculation, the prepared grain substrate was opened under the laminar flow, and five fragments of the isolated fungal culture were placed onto the grain surface. The inoculated bags were incubated in darkness at ambient temperature for a duration of 2 weeks.

2.4. Composite fabrication

2.4.1. Selection of lignocellulosic fibre material and feed preparation

Three locally available, abundant natural fibres, coconut (*Cocos nucifera*) sawdust, mango (*Mangifera indica*) sawdust, and coir pith (spongy byproduct of the coconut fibre extraction process), were used in this study. The sawdust and coir pith were passed through a 4 mm mesh to eliminate large particles. The fibre materials underwent a soaking process in fresh water for a duration of 24 h, followed by a thorough rinsing with fresh water. The soaked material was then squeezed manually and spread on paper to air dry for 24 h. The fibres were placed into polypropylene bags measuring 175 mm × 325 mm and subjected to autoclaving for 20 min at a temperature of 121 °C. The bags were allowed to cool for a duration of 24 h.

2.4.2. Inoculation and cultivation

All composites for each fungus-substrate combination were prepared from a single growth batch to ensure consistency in this study, with five replicates ($n = 5$) analyzed statistically. The 90% wt (wet weight) of fibres was mixed with 10% wt of mushroom spawn, mixed in a sterilised condition, and labelled. The polypropylene bags were subsequently positioned in a dark growth chamber, where the environment was controlled at 28 °C and maintained at a relative humidity of 90%–95%.

2.4.3. Growing MBCs

Following the incubation in growth chambers for 7 d, the cultivated mycelium was moved from bags to PVC moulds (height 20 mm, diameter 60 mm) to initiate the second growth stage. Before filling them with mycelium, the moulds were surface sterilised using 75% ethanol. The mycelium was then added to the moulds in layers, with each layer being compressed to ensure a compact sample. The filled moulds were covered with a transparent cellophane foil and positioned in a growth chamber maintained at a temperature of 28 °C, in darkness, for a duration of 14 d. The cultivation timeline (7 d in bags + 14 d in moulds) was based on preliminary observations of complete visual colonization, adapted from established protocols (Madusanka et al. 2024b).

2.4.4. Ceasing the growth of composites

As described by Madusanka et al. (2024b), following a 14-day growth phase in the moulds, the composites were removed and weighed both before and after drying, with their diameter and height also recorded. Each composite was dried in a convection oven at 80 °C for 6–8 h until a constant weight was achieved. Drying at 80 °C follows established MBC protocols (Elsacker et al. 2019) to cease growth. While this may affect protein structure, chitin remains stable below 300 °C. The influence of drying protocols on molecular structure and mechanical properties requires further investigation. Dried samples were equilibrated at laboratory conditions (24 °C, ~50% RH) before testing.

2.5. Material characterisation of composites

2.5.1. Morphological analysis

All the composites produced in this study were analysed by visual inspection, while mounted specimens were observed using optical microscopy (ZEISS Stemi 508 stereo microscope with Colour View camera). To observe the development of mycelium in biocomposites, SEM (ZEISS EVO 18 research scanning electron microscope, German) analysis was conducted at the Department of Materials Science, Faculty of Engineering, University of Moratuwa, Sri Lanka. Before testing, samples of the composites were coated with a thin layer of gold using sputtering equipment to ensure clear images of the composites (Jones et al. 2018).

2.5.2. Mechanical characterisation

Compression test: Due to the lack of a universally established testing standard for MBCs, mechanical characterization was performed following the ASTM D638 protocol, following the available literature (Elsacker et al. 2019; Raj et al. 2021). Compression strength testing was carried out on five specimens from each composite type. The tests were performed using a Testometric DBBMTCL-500 kg–1.5–000 machine equipped with a 5 kN load cell, under ambient laboratory conditions (24 °C and approximately 50% relative humidity). The specimens evaluated for compression strength were the same ones previously used in determining dry density. The displacement rate was 5 mm/min, and specimens were compressed up to 20% of the samples' original thickness. The compressive stress (σ) and strain (ε) were calculated using the load-displacement curve using the following formulas (Elsacker et al. 2019).

$$\sigma = \frac{F}{A}[\text{MPa}] \text{ and, } \varepsilon = \frac{\Delta L}{L_0}$$

where:

F represents the compressive force measured in N, A denotes the cross-sectional area of the sample in mm^2, ΔL indicates the displacement of the loading surfaces in mm, and L_0 refers to the initial height of the sample in mm.

The compression set value for each composite was obtained according to the following equation.

$$C = \frac{t_0 - t_i}{t_0 - t_n} \times 100\%$$

where:

C represents the compression set, t_0 denotes the thickness of the specimen before compression, t_i indicates the thickness of the sample after testing, and t_n refers to the final thickness of the sample during testing.

2.5.3. Physical characterisation

2.5.3.1. Moisture content. The moisture content on a wet basis for the composite materials was determined in accordance with ISO 16979:2003 (Raj et al. 2021; Madusanka et al. 2024b) using the following formula:

$$M = \frac{(w_w - w_d)}{w_w} \times 100$$

where:

M represents the moisture content expressed as a percentage, W_w denotes the initial mass in g, and w_d indicates the mass following the drying process in g.

2.5.3.2. Dry density and shrinkage. The dry density of the samples was determined in accordance with ISO 9427:2003 (Raj et al. 2021; Madusanka et al. 2024a) with the following formula:

$$V = \frac{\text{Weight of dry sample (kg)}}{\text{Volume of wet sample } (m^3)}$$

2.5.3.3. Capillary water absorption. Completely dried samples were used to measure the capillary water absorption (CWA). After determining the dry weight of the samples, they were placed in a container and submerged by 5 mm in distilled water. The samples were then weighed at specific intervals of time, after 10 min, 30 min, 60 min, 90 min, 2 h, 4 h, 8 h, and 24 h. The CWA was calculated following ISO 15148:2002(E), with the formula (Wei et al. 2023):

$$C_w = \frac{(m_i - m_d)}{(A \cdot \Delta\sqrt{t_i})}$$

In this context, C_w represents the capillary water absorption coefficient measured in $[kg/(m^2 \cdot min^{0.5})]$. The variable m_i denotes the weight of the specimen at a specific time t_i, expressed in kg, while m_d indicates the dry weight of the specimen, also in kg. A refers to the surface area of the specimen that is in contact with water, measured in m^2, and t_i signifies the time in h. No edge sealing was applied; samples were immersed 5 mm, allowing water contact with all exposed surfaces to assess overall moisture resistance behaviour relevant to packaging applications.

2.5.3.4. Thermogravimetric analysis.

A thermogravimetric analysis was performed using the TGA5500 instrument from TA Instrument Inc., Germany. The temperature varied from 30 °C to 700 °C, with a heating rate of 10 °C/min in a nitrogen (N2) atmosphere. Measurements were conducted utilising less than 10 mg of composite placed in a platinum pan, with an airflow rate of 100 mL/min. The TGA test was also conducted on EPS.

2.5.3.5. Flame retardancy test.

The UL-94 horizontal burning (HB) and vertical burning (V) tests were performed to evaluate the flammability characteristics of five specimens each from mycelium-based materials, along with an expanded polystyrene (EPS) reference sample. Specimens for the UL-94 HB test measured 125 ± 5 mm in length and 13 ± 0.5 mm in width, with thickness not exceeding 13 mm; specimens per were used after conditioning at 23 ± 2 °C and 50% ± 5% relative humidity for 48 h. For the UL-94V test, bar specimens were 125 ± 5 mm long and 13 ± 0.5 mm wide, and also preconditioned similarly. Each specimen was marked with reference lines at 25 mm and 100 mm (HB) from the ignited end (V) to track burn progression.

2.5.4. Chemical characterisation

The functional groups in the biocomposites were identified using Fourier Transform Infrared Spectroscopy (FTIR) (Nicolet iS10, Thermo Scientific, USA) over the range of 4000 to 400 cm^{-1} with a resolution of 1 cm^{-1}. Approximately 5 mg of the sample was ground thoroughly with 95 mg of FTIR-grade potassium bromide (KBr) using an agate mortar and pestle with precautions taken against moisture absorption, and the mixture was compressed using a manually operated die to form the sample pellet.

2.5.5. Soil burial test

A soil burial experiment, adapted from the method outlined by Namphonsane et al. (2023), was conducted to evaluate the microbial biodegradability of the biocomposites. Specimens with a diameter of 20 mm were fabricated specifically for this test. Commercial compost was used at ambient temperature (~28 °C), with a pH of 6.8 and a moisture content of 55%. Each sample was enclosed in a nylon mesh, weighed, and placed within a 20 L compost container.

The trial was carried out over 30 d. Samples were examined on days 7, 15, and 30. After 30 d, all specimens were oven-dried at 40 °C until a constant mass was achieved. Biodegradability was further assessed through visual inspection of the specimens.

2.5.6. Comparative analysis using Ashby chart

To visually assess the performance of various materials, distinct combinations of attributes (e.g., strength, density) were represented on a material property chart (often referred to as an Ashby chart) using a log-log scale (Ashby 2011). Mycelium-based composites exhibit properties comparable to those of foams, natural materials, and conventional synthetic insulation products, including rock wool, cork, sheep wool, high-density polyurethane (HDPU), and expanded polystyrene (EPS) (Akromah et al. 2024; Whabi et al. 2024).

2.6. Statistical analysis

The statistical analysis of moisture content, dry density, capillary water absorption, and compression set was conducted using Minitab 21 (version 3.1), and the results were visualised with Origin Pro 2022 (version 9.9.0.22). The data collected were subjected to one-way analysis of variance (ANOVA), and the significant means were distinguished by mean differences utilising the Tukey test at $\alpha = 0.05$.

3. Results and discussion

3.1. Fungal sampling, spawn preparation, and substrate preparation

Species identification was confirmed through integrative taxonomy combining molecular data (ITS sequences with 99%–100% similarity to reference sequences), macro-morphological characteristics matching the protologue or recently published descriptions, and available ecological data. The BLAST search of the ITS sequences derived from CM17 (GenBank: PP987317) revealed that the isolate used in this study is *Ganoderma orbiforme* (GenBank: PV59611), with 99.65% similarity and a 100% query coverage. This species was originally described from Guinea (Fries 1836) and recently reported from Sri Lanka by Konara et al. (2024). Macro-morphology of the *G. orbiforme* also aligned with the protologue and recent morphological descriptions available. Similarly, ITS sequence derived from M34 (GenBank: PP001103) revealed that the isolate used in this study is *Lentinus squarrosulus* (GenBank: OP758152) with 100% similarity and query coverage, and morphological similarity available in the protologue and recent publications (Kandagalla and Krishnappa 2020; Miriyagalla et al. 2022). Therefore, the two mushrooms used for the isolation of mycelia were confirmed as *G. orbiforme* (CM17) and *L. squarrosulus* (M34) based on molecular data and morphology.

3.2. Growth evaluation and fabrication of mycelium-based biocomposites

In the visual inspection, a dense white layer of mycelium was observed in the combinations of CM17 inoculated coconut sawdust (CSG), mango sawdust (MSG), coir pith (CPG), and M34 inoculated coir pith (CPL). A thin white mycelium layer was observed on mango sawdust inoculated with M34 (MSL), as shown in Figure 1. Additionally, CM17 showed a higher growth rate than M34 during the growth phase.

This difference in growth rates can be explained by strain-specific enzymatic activity and metabolic profiles that affect the capacity to degrade lignocellulosic substrates efficiently. *Ganoderma* species, including *G. orbiforme*, are recognized for producing a diverse array of lignin-modifying enzymes such as laccases, manganese peroxidases, and versatile peroxidases, which facilitate effective breakdown of lignin and cellulose structures in woody substrates (Thiribhuvanamala and Krishnamoorthy 2021). This enzymatic versatility enhances colonisation and nutrient assimilation, supporting faster mycelial expansion on lignocellulose-based materials.

Shapes and sizes of the test samples (60 mm × 20 mm cylinders) enabled standardized testing. When the samples are made in different sizes, larger than the test samples, some properties may reflect the impact of oxygen/nutrient gradients and colonization heterogeneity. Industrial-scale production with optimized mould designs and process controls represents a critical next step toward commercialization.

In contrast, *Lentinus squarrosulus* produces a suite of biomass-degrading enzymes, including glycoside hydrolases and auxiliary activity enzymes. Still, its enzymatic expression can be influenced significantly by substrate type and environmental conditions (Onyeka et al. 2025). Transcriptomic studies reveal the complexity and regulation of ligninolytic enzymes in *L. squarrosulus*, which may contribute to its relatively slower mycelial growth compared to *G. orbiforme*, depending on substrate compatibility and nutrient availability (De Leon et al. 2017; Thiribhuvanamala and Krishnamoorthy 2021).

The comparison of freshly prepared and dried composite revealed that the CPG composite achieved the highest shrinkage (40.9%) and had the highest density (Table 1). The CSG recorded the lowest shrinkage percentage (5.4%). The shrinkage percentage is slightly higher for composites fabricated with coir pith (28.3% and 40.9%) than coconut (5.4%) and mango sawdust (14.6% and 22.9%). The observed results may be linked to the significant water absorption capacity of the coir pith. It is highly absorbent and can retain water up to 8–10 times its weight. Typically, 1 kg of dry coir pith can absorb around 5–8 L of water (Prakash et al. 2021).

3.3. Morphological analysis

Different visual characteristics were observed in the five composites produced. The CSG and CPG composites showed similarities in colour and texture. The

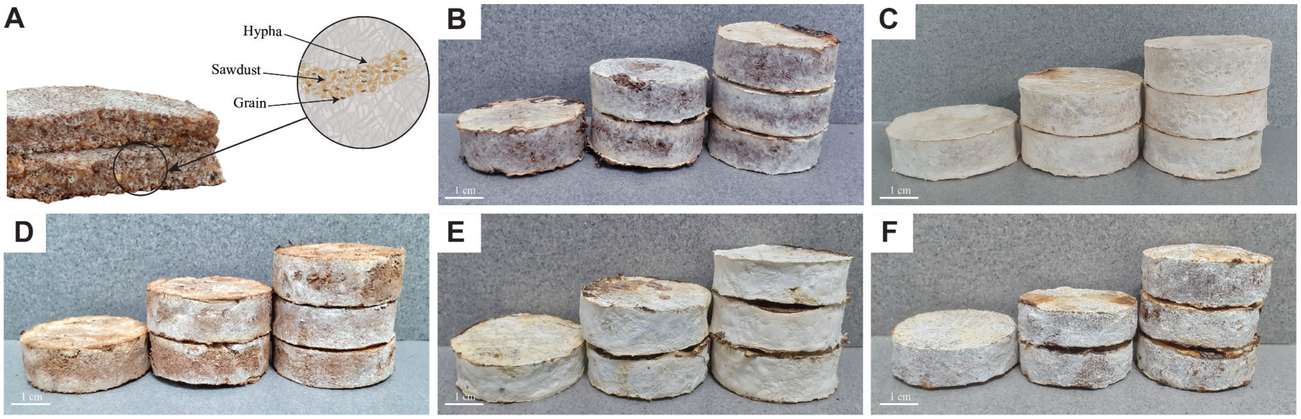

Figure 1. Mycelium-based composites produced during this study after drying. (A) Cross-sectional image of MSL. (B) CSG: *Ganoderma orbiforme* + coconut sawdust. (C) MSG: *G. orbiforme* + mango sawdust. (D) MSL: *Lentinus squarrosulus* + mango sawdust. (E) CPG: *G. orbiforme* + coir pith. (F) CPL: *L. squarrosulus* + coir pith.

CSG, CPG, and CPL composites were relatively soft and foamy, while the MSG and MSL appeared to have a rough surface texture upon visual inspection. Thus, mango sawdust resulted in better growth compared to coir pith composites in terms of the density of mycelium. Compared to coir pith composites, mango sawdust produced a rough surface texture. CM17 grown on mango sawdust formed a velvety and smooth skin at the substrate surface. The visual examination of the composites revealed that fungal colonisation was more extensive and denser throughout MSG, CPG, and CPL composites compared to CSG and MSL. Stereo microscopy analysis of a cross-section of CSG, CPG, and MSL revealed that fungal colonisation was more concentrated near the surfaces of the composites in comparison to the centre of the composites. The MSG and CPL composites had dense fungal colonisation in the centre. Appels et al. (2019) have shown that mycelium growth in the centre of the composite can be improved by increasing the oxygen level in the centre of the material.

The stereomicroscopy and SEM images of mycelium-based biocomposites are shown in Figure 2. According to the stereomicroscopic imaging, the hyphae had completely occupied the area between the sawdust and coir pith particles on the outer surface of the material. The SEM images of the composites revealed that the MSG and CPL composites have higher fungal colonisation than the other samples produced in this study. The dried composites showed colour variation, with white to brown patches. As described by Antinori et al. (2020), the brown patches are likely a result of non-enzymatic browning due to the sugars and proteins present in the fungal cell walls and the plant material. Previous research suggests oxygen availability may influence central colonization (Appels et al. 2019). While our moulds were covered with gas-permeable cellophane, a systematic comparison of different aeration strategies was not conducted.

3.4. Thermogravimetric analysis

The thermal decomposition of mycelium biocomposites consisted of three decomposition phases, which were similar to those of previous studies (Appels et al.

Table 1. Summary of moisture content, dry density, average shrinkage, and compressive strength of produced biocomposites.

Code	Initial moisture content (%)	Dry density (kg/m^3)	Average shrinkage (%)	Compressive strength (MPa)
CSG	36.5 ± 3.6^c	379.3 ± 45.4^b	5.4 ± 2.8^d	0.34 ± 0.01^c
MSG	59.5 ± 0.9^a	286.8 ± 28.2^c	22.9 ± 2.9^b	0.65 ± 0.05^a
MSL	54.8 ± 4.9^{ab}	306.3 ± 44.9^{bc}	14.6 ± 4.3^c	0.35 ± 0.02^c
CPG	45.8 ± 2.9^{bc}	474.7 ± 55.7^a	40.9 ± 3.1^a	0.14 ± 0.01^d
CPL	60.3 ± 9.2^a	274.1 ± 60.3^c	28.3 ± 2.8^b	0.48 ± 0.04^b
CSL	N/A*	N/A*	N/A*	N/A*
EPS	N/A	13.4 ± 2.1^d	N/A	0.07 ± 0.01^e

The standard deviation is calculated with five replicates (mean ± one standard deviation). Letters (a, b, c, d, e) indicate significant differences based on Tukey's family error rate at $p < 0.05$ for sample-specific ANOVA. *Specimens failed to grow, N/A = Not applicable. CSG: *Ganoderma orbiforme* + coconut sawdust; MSG: *G. orbiforme* + mango sawdust; MSL: *Lentinus squarrosulus* + mango sawdust; CPG: *G. orbiforme* + coir pith; CPL: *L. squarrosulus* + coir pith; CSL: *L. squarrosulus* + coconut sawdust; EPS: Expanded polystyrene.

2019; Gou et al. 2021). The first stage of decomposition was the evaporation of moisture, where the temperature ranged from 30 °C to 105 °C (Figure 3). Heating biocomposites causes a weight reduction due to the release of bound water and volatile extractives. This is a common occurrence in plant fibres and results in increased flexibility and collapsibility of the fibres, especially under compression (Namphonsane et al. 2023). Gou et al. (2021) have confirmed that the thermal degradation of lignocellulose and the production of elementary residual products from lignocellulosic fibres are associated with the second and third phases. In the second stage, compared with MSG, which started to degrade at around 220 °C [initial rise (T_{on}) in Table 2], with a maximal degradation temperature of 340 °C (T_{P2}), the thermal degradation onset of MSL occurred at a higher temperature at 233 °C (T_{on}), with one degradation peak at 363 °C (T_{P2}). Although the CPG and CPL show similar mass loss (39%) (not shown here) during 183–391 °C and 193–373 °C, respectively, the CPL shows 44% mass loss at ≥ 373 °C while CPG shows only 27% mass loss at ≥ 391 °C. The higher thermal stability of CPG based on *Ganoderma* sp. may be attributed to greater chitin content, as suggested by FTIR analysis (peak at 1374 cm^{-1}) (Sun et al. 2019). Generally, chitin is known to be more thermally stable than lignin and is likely to decompose at a higher temperature (Sun et al. 2019). The increase in thermal stability (lower mass loss) is proposed to be caused by the decomposition of hemicellulose, lignin, and other more stable components by fungi (Alaux et al. 2024; Majib et al. 2025). The thermal stability difference between CPG and CPL can be primarily attributed to the influence of the strains of fungi involved in their decomposition. This is because both CPG and CPL are made of the same fibre material, but the specific fungi strains that break down the fibres can have different enzymatic capabilities and, therefore, different effects on the thermal stability of the resulting products.

The results obtained were compared with those of thermogravimetric properties for EPS. The findings of this TGA analysis indicate that the mycelium biocomposites tested had lower thermal stability than EPS (expanded polystyrene), but they also produced a higher residue mass. These results suggest that the mycelium biocomposites could be a viable option for producing lightweight materials, which are in high demand for packaging applications. Furthermore, the results demonstrated that the produced biocomposites (except CPL) have an advantage over EPS as insulation materials at temperatures of up to 450 °C, as EPS underwent rapid decomposition under similar conditions. This suggests that these biocomposites could be a more suitable option for applications that require insulation materials to withstand higher temperatures.

3.5. Capillary water absorption

The capillary water absorption coefficient (C) was obtained in the first 90 min, as shown in Figure 4A. The MSL [4.49 kg/(m^2•$h^{0.5}$)] has stronger water absorbent properties than CSG [2.16 kg/(m^2•$h^{0.5}$)] and MSG [2.75 kg/(m^2•$h^{0.5}$)] composites. Both CPG and CPL composites using coir pith substrate exhibited water-repellent properties ($C < 0.5$) regardless of fungal species, suggesting substrate type as a dominant factor. The absorption of capillary water can be affected by the type of substrate, which aligns with the research findings of Walker and Pavia (2014). Additionally, capillary water absorption correlates with the amount of fungal colonisation (Vašatko et al. 2022; Wei et al. 2023). The MSL composite had very low fungi colonisation and strong water-absorption properties. The CPG composite has the highest dry density and water-repellent properties. Although the CPL had the lowest dry density, it also shows water-repellent properties. The reason for this could be the dense fungal colonisation. The MSG composite, which exhibits better mechanical properties, has water-absorbing properties, which may need the application of surface coating in further development.

3.6. Compressive strength

Given the lack of a universally accepted testing protocol for MBCs, an initial phase of experimentation was conducted, whereby various mould shapes were tested, based on existing literature (Elsacker et al. 2019). Then, a diameter-to-height ratio of 3:1 was selected for the compression test. To determine the 20% relative deformation value, the maximum force required to displace the sample by 20% is measured. A higher compressive strength is typically desirable as it indicates that the material can withstand higher compressive loads before deforming or failing. Therefore, materials with higher compressive strength values are generally considered more

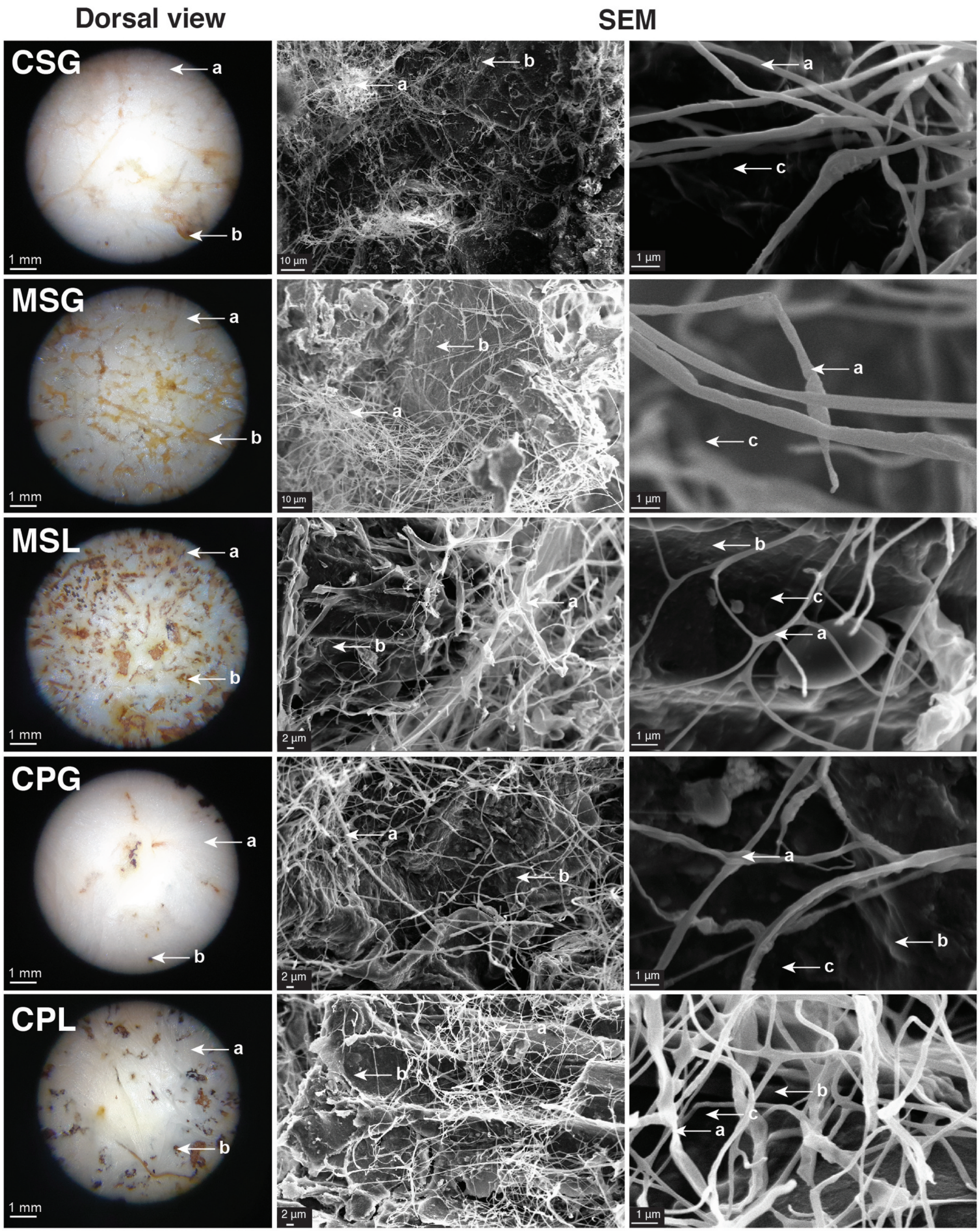

Figure 2. Stereomicroscopy and scanning electron microscopy (SEM) images of mycelium-based biocomposites. Arrows indicate mycelium (a), substrate (b), and air voids (c). CSG: *Ganoderma orbiforme* + coconut sawdust; MSG: *G. orbiforme* + mango sawdust; MSL: *Lentinus squarrosulus* + mango sawdust; CPG: *G. orbiforme* + coir pith; CPL: *L. squarrosulus* + coir pith.

valuable. The samples with uniformly colonised and dense white fungal biomass showed the highest compressive strength (Table 1). Lignin is the molecule responsible for the strong bonding force between the cell walls of mycelium composites (Alaux et al. 2024; Majib et al. 2025). As a result, the bonding between mycelium and lignin can be stronger, contributing to stronger overall bonds in mycelium composites (Shin et al. 2025).

The MSG composite achieved the highest compressive strength (0.65 MPa), followed by the CPL composite (0.48 MPa). The lowest compressive strength is recorded by the CPG composite (0.14 MPa). The CPG and CPL composites were produced with the same substrate but with different fungal strains; thus, the difference in compressive strength is caused by the effects of the fungal strain. Additionally, the MSG and MSL composites were

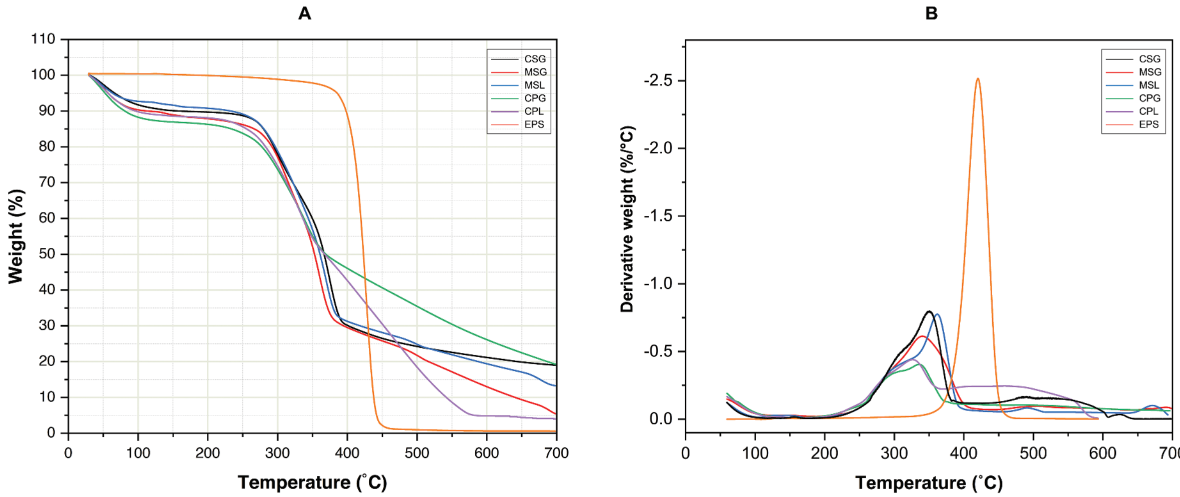

Figure 3. Rate of mass change from TGA (thermogravimetric analysis) (A) and DTGA (differential thermogravimetric analysis) curves of mycelium-based biocomposites (B). CSG: *Ganoderma orbiforme* + coconut sawdust; MSG: *G. orbiforme* + mango sawdust; MSL: *Lentinus squarrosulus* + mango sawdust; CPG: *G. orbiforme* + coir pith; CPL: *L. squarrosulus* + coir pith; EPS: Expanded polystyrene.

Table 2. Onset and peak temperatures of thermal degradation of mycelium-based composites and EPS.

Biocomposite	T_{on} (°C)	T_{p1} (°C)	T_{p2} (°C)
CSG	244.39	316.50	349.15
MSG	220.05	301.21	340.87
MSL	233.63	312.29	363.34
CPG	192.06	303.63	334.44
CPL	193.96	294.60	327.71
EPS	321.35	420.91	–

T_{on} refers to the onset temperature. The degradation temperatures, T_{P1} and T_{P2} refer to the different peak temperatures observed on the DTG curves and are related to the different thermal degradation steps for each composite. CSG: *Ganoderma orbiforme* + coconut sawdust; MSG: *G. orbiforme* + mango sawdust; MSL: *Lentinus squarrosulus* + mango sawdust; CPG: *G. orbiforme* + coir pith; CPL: *L. squarrosulus* + coir pith; EPS: Expanded polystyrene.

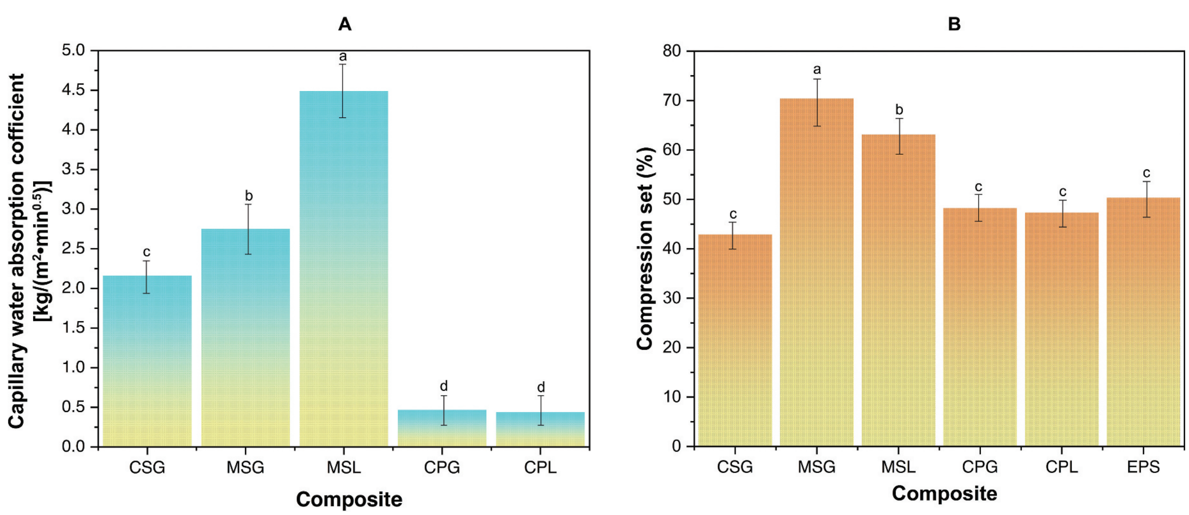

Figure 4. Capillary water absorption coefficient (A) and compression set of the mycelium-based composites (B). CSG: *Ganoderma orbiforme* + coconut sawdust; MSG: *G. orbiforme* + mango sawdust; MSL: *Lentinus squarrosulus* + mango sawdust; CPG: *G. orbiforme* + coir pith; CPL: *L. squarrosulus* + coir pith; EPS: Expanded polystyrene; letters (a, b, c, d) indicate significant differences based on Tukey's family error rate at $p < 0.05$ for sample-specific ANOVA.

produced with *Mangifera indica* sawdust, but with two different fungi strains. While the MSG composite shows the highest strength (0.65 MPa) the MSL composite shows a lower value (0.35 MPa). The findings indicate that CM17 and M34 exert a notable influence on the compressive strength. Higher density does not always mean higher compressive strength. The MSG composite presents the highest value of compressive strength (0.65 MPa) while presenting an average dry density of 286.76 kg/m^3. The CPG composite had the highest average value of dry density (474.72 kg/m^3) while presenting the lowest compressive strength of 0.14 MPa.

While statistical analysis revealed significant differences among composites ($p < 0.05$, Table 1), practical significance for packaging applications depends on minimum performance thresholds. Several composites with statistically different strengths may be equally suitable for specific applications.

Products with lower density and higher compressive strength are generally considered to have greater value. This is because lighter materials are easier to transport and use in various applications in terms of packaging and insulation (Shin et al. 2025). Therefore, the MSG and CPL composites can be considered the most relevant since they have a low density and a relatively high compressive strength.

Observed variability in compressive strength (Table 1) reflects inherent biological heterogeneity and manual processing methods common in laboratory-scale MBC production. Process standardisation and automation would be necessary to achieve industrial consistency, as observed in commercial MBC manufacturers (Robertson 2020).

3.7. Compression set

The compression set is a parameter used to assess how well an elastomeric material can regain its original size and shape after being compressed. This study is the first reported compression set on mycelium composites. Due to the absence of a standardised testing method for mycelium-based composites, the compression set testing followed ASTM D395 Method B with compression to 75% original thickness, performed at 24 °C and 50% relative humidity, with thickness measured within 30 s after load release. The compression set is determined as the percentage difference between the composites' original thickness and thickness after testing relative to the amount of deflection applied during testing. In simpler terms, these values indicate the material's ability to recover its initial thickness.

It is necessary to maintain the shape and functionality of biocomposites over time, and the compression set is a crucial parameter to evaluate their ability to recover their initial thickness. A low compression set value indicates that the material can recover efficiently from compression and sustain its performance over an extended period. In contrast, a high compression set value implies that the material may undergo permanent deformation and deteriorate over time. Thus, the compression set is a significant parameter to consider when assessing the long-term performance of materials in applications where they will encounter compressive loads.

As shown in Figure 4B, the CSG composite exhibits the lowest compression set (42.88%). The CPL and CPG composites, which were made from the same lignocellulosic material, also have low compression set values (47.35% and 48.22%). Those composites can recover efficiently from compression and sustain their performance over an extended period. The compression set of CPG and CPL composites is comparable to commercial EPS (50.35%) tested under identical conditions. On the contrary, MSG and MSL had the highest compression set values (70.46% and 63.15%). These results indicate that the fungal strain has little effect on the compression set of fungal composites and that the lignocellulosic matrix is more influential on this characteristic.

3.8. FTIR analysis

The overall composition of different substrates was analysed through an FTIR analysis, which involved observing the appearance and disappearance of certain bands. The FTIR spectra of both fungal-colonised and original fibres were recorded. FTIR analysis revealed qualitative differences in functional groups between substrates, mycelium, and composites. The spectral changes suggest substrate modification by fungal enzymes, consistent with reported ligninolytic capabilities of fungal species (Thiribhuvanamala and Krishnamoorthy 2021).

The FTIR spectrum of the CPL composite was compared to that of the fresh coir pith and with pure mycelium grown on the coir pith (Figure 5A). The peak presence in 3437 cm^{-1}, which corresponds to O-H stretching, indicates a strong presence of hydroxyl groups, likely due to abundant carbohydrates in undecayed coir pith. In 2930 cm^{-1}, the peak indicates C-H stretching in lipids. In the composite, the spectrum also revealed an increase in the relative intensities attributed to the aromatic (C=C) of lignin at1510 cm^{-1}, 1456 cm^{-1}, and the C-O bond at 1262 cm^{-1} compared to fresh coir pith. In addition, the mycelium spectrum indicated the presence of a peak at 1374 cm^{-1}, which was assigned to C-H bonding in the chitin and differed from fresh coir pith. Chitin is a structural polysaccharide that influences the physical strength of mycelium-based composites (Elsacker et al. 2019; Zhou et al. 2020).

The FTIR spectrum of the MSG composite was also compared to that of the fresh mango sawdust and pure mycelium grown on mango sawdust, as shown in Figure 5B. The degradation of the MSG composite by CM17 led to a small decrease in intensities at 3437 cm^{-1}, suggesting hydroxyl groups in cellulose and hemicellulose in the plant material. The degradation of mango sawdust also resulted in increased intensities at 1510 cm^{-1}, 1456 cm^{-1}, and 1262 cm^{-1} attributed to aromatic rings, C-H deformation, and aromatic methoxyl group in lignin, respectively. The spectrum of the MSG composite indicated the presence of a clear peak at 1374 cm^{-1}, which was assigned to chitin.

Overall, in undecayed mango sawdust, dominated by lignin, reflecting its plant-based composition. The spectrum of the mycelium shows a notable protein signature and minimal lignin, consistent with fungal biomass rich in polysaccharides and proteins. The spectrum of the composite combines features of both, with a balanced profile of hydroxyl groups, carbohydrates, lignin, and proteins.

A low vibrational frequency of 2930 cm^{-1} (within the 2800 cm^{-1} to 3000 cm^{-1} range) is indicative of a lipid-based structure. In contrast to cellulose, the mycelium more readily absorbs feeding substrates such as starch and glucose, which promotes the biosynthesis of lipids rather than chitin. Past research has indicated that the breakdown of lignin, which is caused by phenol-oxidising enzymes (specifically laccase and peroxidase), impacts the adhesion and strength of composites. These enzymes encourage the formation of cross-links between lignin-based radicals, which increases the composite's strength. Additionally, a greater quantity of cellulose in fibres leads to higher Young's modulus and tensile strength (Elsacker et al. 2019; Madusanka et al. 2024a). The compressive strength of mango sawdust-based composites (MSG) was found to be higher (0.65 MPa) than that of coir pith-based composites (0.48 MPa). In summary, the test results demonstrate that the mechanical performance of mycelium-based composites is predominantly affected by the type of fibre incorporated.

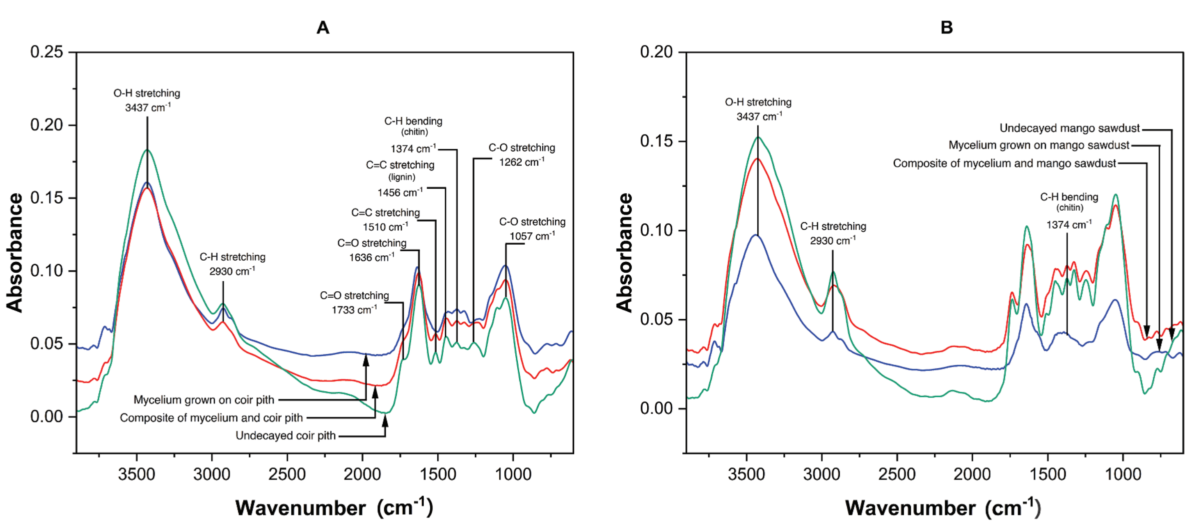

Figure 5. FTIR spectra of mycelium composites. (A) CPL: *Lentinus squarrosulus* + coir pith. (B) MSG: *Ganoderma orbiforme* + mango sawdust.

3.9. Fire resistance

Table 3 shows that all biocomposites except EPS reach the UL-94 V1 vertical burning classification, while EPS fails to achieve any vertical rating and exhibits a much higher horizontal burning rate. The CSG, MSG, MSL, CPG, and CPL biocomposites present low horizontal burning rates, varying around 28–33 mm/min, and all are classified as V1 in the UL-94 vertical test, indicating self-extinguishing behaviour with limited dripping and after-flame time. In contrast, EPS shows a burning rate of about 110 mm/min, more than three times higher than the biocomposites, and does not attain a UL-94 V rating, reflecting rapid flame spread and poor fire resistance. Due to their better flame-retardant performance, mycelium-based biocomposites represent a promising alternative to expanded polystyrene for applications where enhanced fire safety is required.

Table 3. The UL-94 horizontal burning (HB) and vertical burning (V) test results of biocomposites.

Biocomposite	Burning rate (mm/min)	UL-94V rating
CSG	29.70 ± 0.32^{c}	V1
MSG	28.00 ± 0.35^{d}	V1
MSL	28.20 ± 0.50^{cd}	V1
CPG	32.67 ± 0.70^{b}	V1
CPL	32.03 ± 0.45^{b}	V1
EPS	110 ± 2.06^{a}	Not achieved

Letters (a, b, c, d) indicate significant differences based on Tukey's family error rate at $p < 0.05$ for sample-specific ANOVA. CSG: *Ganoderma orbiforme* + coconut sawdust; MSG: *G. orbiforme* + mango sawdust; MSL: *Lentinus squarrosulus* + mango sawdust; CPG: *G. orbiforme* + coir pith; CPL: *L. squarrosulus* + coir pith; EPS: Expanded polystyrene.

3.10. Environmental implications

All biocomposites completed the degradation cycle within 1 month, as indicated by the soil burial test findings (Figure 6). After 7 days, brown stains appeared on the surfaces while the biocomposites still retained their original shapes. By day 15, the materials had fragmented into small pieces, and by day 30, the lignocellulosic components had separated from the binding hyphae and were partially decomposed. This demonstrates that the total disintegration time for the substrate from the composites is 30 days, which is sufficient for complete disintegration. The MSG composite exhibited lower compostability relative to the other samples. Visual assessment confirmed that all biocomposites produced in this study are capable of undergoing composting.

While biodegradability suggests environmental advantages over EPS, a comprehensive life cycle assessment including energy inputs, carbon footprint, and end-of-life analysis would provide quantitative validation of sustainability claims (Alaux et al. 2024).

3.11. Comparison with conventional materials

According to the Ashby chart generated in this study (Figure 7), the mycelium composites (CSG, MSG, MSL, and CPL) behave similarly to cork and low-density foams. This makes them suitable for insulating, cushioning, and sustainable design applications, but not for structural use. This is the first study to report a comparison between its own mycelium-based composite data and a material property chart.

Except for the CPG composites, all other combinations overlap with the foam region. Hence, they will be a viable option for the packaging industry because low strength is acceptable, and low density is an advantage. Achieving lower density can increase the market value for biocomposites. By reducing the weight of the material, transportation costs can be lowered, and the product can become more appealing to customers who value environmentally friendly alternatives. Due to their biodegradability, it is suitable for eco-friendly single-use packaging to replace polystyrene or polyethylene. Since the foam materials are used as acoustic insulation and thermal insulation, our composites will be eco-friendly applications in those industries. The lightweight, aesthetic appeal, and natural texture of the biocomposites make them suitable for use in eco-interior cladding, wall panels, and furniture accents (Akromah et al. 2024). Additionally, the biodegradability of the biocomposites will be a viable application in electronic packaging, disposable containers, and molded inserts used to secure products inside boxes. Long-term mechanical behaviour, including creep, stress relaxation, and fatigue performance under cyclic loading, represents important areas for future investigation to fully assess packaging application suitability.

EPS used in this study was of Standard Light (SL) grade, which is commonly employed for general packaging applications. The approximate density is 13.5 kg/m^3. Notably, the compression set of the tested EPS sample was 50.35% during this study. Similar compression set values were recorded for CPG and CPL

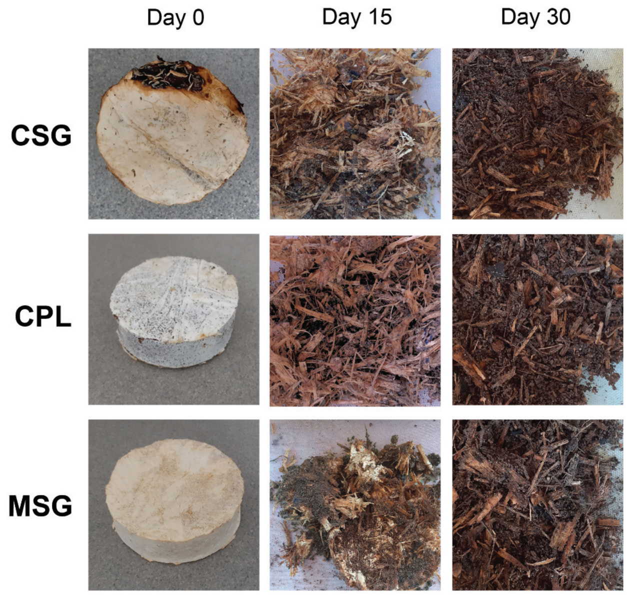

Figure 6. Visual observations from the soil burial test at days 0, 15, and 30. CSG: *Ganoderma orbiforme* + coconut sawdust; CPL: *Lentinus squarrosulus* + coir pith; MSG: *G. orbiforme* + mango sawdust.

composites. These results revealed that the CPG and CPL composites are compatible with commercial EPS.

This approach allows for the identification of optimal combinations for producing MBCs with physical and mechanical properties comparable to or superior to EPS, introducing a novel and sustainable solution in the packaging industry.

The estimated production cost of the specific mycelium-based composites developed in this study was approximately 0.5 USD per kilogram, including the sterilization and drying processes. However, it is anticipated that large-scale production and process optimisation will substantially reduce the unit cost. At present, mycelium-based materials are often positioned as premium, environmentally conscious, innovative products. To make these materials more accessible for widespread packaging applications, scaling up production will be essential to achieve cost competitiveness with conventional materials. Reinforcement packaging material with natural fibre

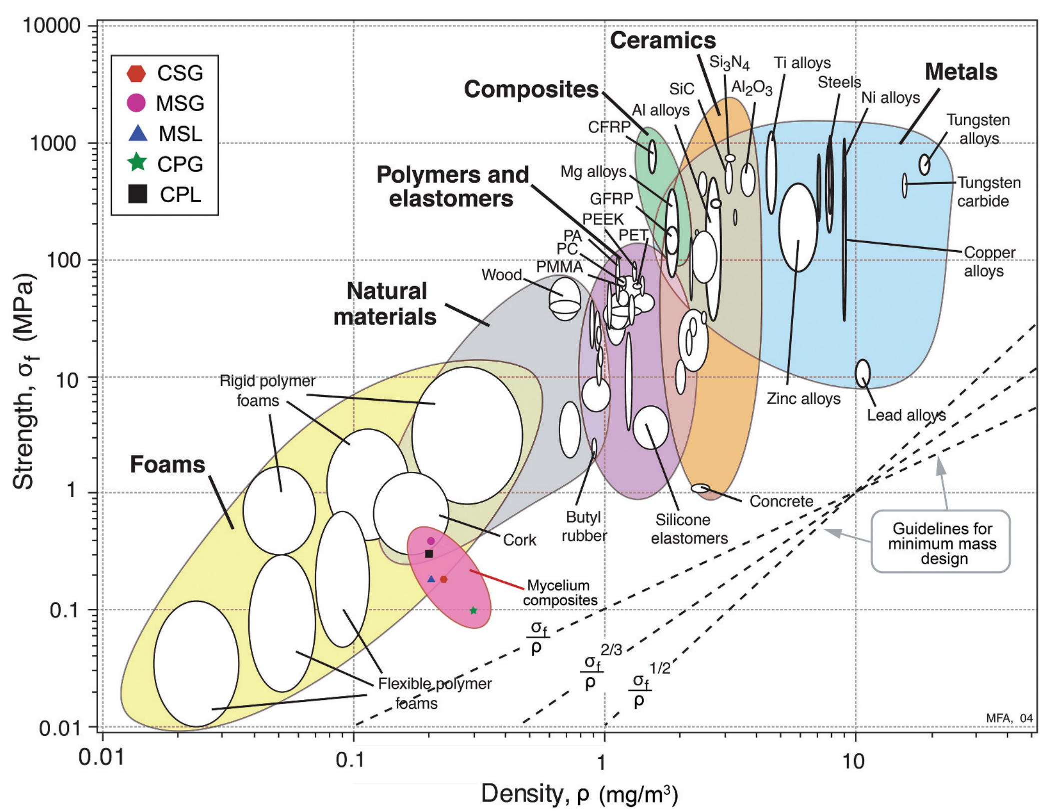

Figure 7. Material property chart comparing mycelium-based composites to material families. Background material zones (foams, polymers, cork, etc.) are from established databases (Ashby 2011). Experimental MBC data from this study are plotted as individual points. CSG: *Ganoderma orbiforme* + coconut sawdust; MSG: *G. orbiforme* + mango sawdust; MSL: *Lentinus squarrosulus* + mango sawdust; CPG: *G. orbiforme* + coir pith; CPL: *L. squarrosulus* + coir pith.

combinations will drastically enhance the strength in larger panels while keeping the cost reasonably lower (Kohphaisansombat et al. 2024).

This study has some limitations that should be addressed by future research when the materials are produced in large scale with various application-specific characteristics. Despite these constraints, the study offers a valuable baseline characterization of novel fungus-substrate combinations and establishes a foundation for systematic optimization and future pre-commercial development.

4. Conclusions

This study demonstrates the potential of mycelium-based composites (MBCs) fabricated using locally sourced fungi *G. orbiforme* (CM17) and *L. squarrosulus* (M34) and commonly available plant biomass as sustainable alternatives to synthetic materials. The incorporation of CM17 with coir pith and M34 with coconut sawdust resulted in MBCs exhibiting physical and mechanical properties that are comparable to, or in some cases surpass, those of Standard Light (SL) grade expanded polystyrene. Coir pith-based composites containing both fungal strains showed very low water absorption coefficients, suggesting their suitability for a range of applications. The high fixed carbon content in the biocomposites highlights their potential for use in insulation and interior applications. The combination of coir pith and CM17 shows similar compressive strength to EPS. Mycelium composites with a compressive strength of 0.65 MPa and a dry density of 286.8 kg/m^3 behaved similarly to cork and low-density foams. Among combinations tested, MBCs made with coir pith and coconut sawdust show potential as eco-friendly alternatives for protective packaging applications. A thorough evaluation of the diverse properties of mycelium-based composites (MBCs) provides insights into the advancement of green manufacturing and aligns well with global initiatives towards promoting circular bioeconomy solutions.

Acknowledgments

The authors thank the University of Sri Jayewardenepura (USJ) for facilitating and funding fungal biotechnology research.

Disclosure statement

No potential conflict of interest was reported by the author(s). The use of trade names is solely to provide specific information.

Funding

This research is supported by the University of Sri Jayewardenepura (USJ) through the grant [ASP/01/RE/TEC/2022/67].

Data and availability

The authors declare that the data supporting the findings of this study are available within the paper. Should any raw files of images be needed in another format, they are available from the corresponding author upon reasonable request. Source data are provided in this paper.

Author contributions

CRediT: **Chathura Madusanka:** Formal analysis, Writing – original draft; **Dhanushka Udayanga:** Conceptualization, Data curation, Funding acquisition, Investigation, Methodology, Project administration, Resources, Supervision, Validation; **Renuka Nilmini:** Data curation, Resources, Supervision, Writing – review & editing; **Suranga Rajapaksha:** Resources, Supervision, Writing – review & editing; **Choolaka Hewawasam:** Data curation, Project administration, Resources, Supervision; **Dimuthu Manamgoda:** Data curation, Project administration, Resources, Writing – review & editing; **Indunil S. Herath:** Resources, Writing – original draft; **Mapa Mudiyanselage Sumudu Tharangani Mapa:** Project administration, Supervision, Writing – review & editing; **Juliana Vasco-Correa:** Project administration, Supervision, Validation, Visualization, Writing – review & editing.

References

Akromah S, Chandarana N, Eichhorn SJ. 2024. Mycelium composites for sustainable development in developing countries: the case for Africa. Adv Sustainable Syst. 8 (1):2300305. doi: 10.1002/adsu.202300305.

Alaux N, Vašatko H, Maierhofer D, Saade MRM, Stavric M, Passer A. 2024. Environmental potential of fungal insulation: a prospective life cycle assessment of mycelium-based composites. Int J Life Cycle Assess. 29(2):255–272. doi: 10.1007/s11367-023-02243-0.

Alemu D, Tafesse M, Mondal AK. 2022. Mycelium-based composite: the future sustainable biomaterial. Int J Biomater. 2022(1):1–12. doi: 10.1155/2022/8401528.

Appels FV, Camere S, Montalti M, Karana E, Jansen KM, Dijksterhuis J, Krijgsheld P, Wösten HA. 2019. Fabrication factors influencing mechanical, moisture-and water-related properties of mycelium-based composites. Mater Des. 161:64–71. doi: 10.1016/j.matdes.2018.11.027.

Ashby MF. 2011. Material selection in mechanical design. Kidlington: Oxford; p. 54.

Attias N, Danai O, Abitbol T, Tarazi E, Ezov N, Pereman I, Grobman YJ. 2019. Mycelium bio-composites in industrial design and architecture: comparative review and experimental analysis. J Cleaner Prod. 246:119037. doi: 10.1016/j.jclepro.2019.119037.

Arnold AE, Lutzoni F. 2007. Diversity and host range of foliar fungal endophytes: Are tropical leaves biodiversity hotspots? Ecology. 88(3):541–549. doi: 10.1890/05-1459.

Antinori ME, Ceseracciu L, Mancini G, Heredia-Guerrero JA, Athanassiou A. 2020. Fine-tuning of physicochemical properties and growth dynamics of mycelium-based materials. ACS Appl Bio Mater. 3(2):1044–1051. doi: 10.1021/acsabm.9b01031.

Bhardwaj A, Alam T, Sharma V, Alam MS, Hamid H, Deshwal GK. 2020. Lignocellulosic agricultural biomass as a biodegradable and eco-friendly alternative for polymer-based food packaging. J Packag Technol Res. 4:205–216. doi: 10.1007/s41783-020-00089-7.

Bravo A, Hotchkiss JH. 1993. Identification of volatile compounds resulting from the thermal oxidation of polyethylene. J Appl Polym Sci. 47:1741–1748. doi: 10.1002/app.1993.070471004.

De Leon AM, Guinto LJZG, De Ramos PDV, Kalaw SP. 2017. Enriched cultivation of *Lentinus squarrosulus* (Mont.) Singer: a newly domesticated wild edible mushroom in the Philippines. Mycosphere. 8(3):615–629. doi: 10.5943/mycosphere/8/3/9.

Dhiman S, Kaur P, Narang J, Mukherjee G, Thakur B, Kaur S, Tripathi M. 2024. Fungal bioprocessing for circular bioeconomy: exploring lignocellulosic waste valorization. Mycology. 15(4):538–563. doi: 10.1080/21501203.2024.2316824.

Elsacker E, Vandelook S, Brancart J, Peeters E, De Laet L. 2019. Mechanical, physical and chemical characterisation of mycelium-based composites with different types of lignocellulosic substrates. PLOS One. 14(7):e0213954. doi: 10.1371/journal.pone.0213954.

Fries EM. 1836. Anteckningar öfver de i Sverige växande ätliga svampar [notes on the edible mushrooms growing in Sweden]. Uppsala, Sweden: Palmblad, Sebell; p. 1–50.

Gou L, Li S, Yin J, Li T, Liu X. 2021. Morphological and physico-mechanical properties of mycelium biocomposites with natural reinforcement particles. Constr Build Mater. 304:e124656. doi: 10.1016/j.conbuildmat.2021.124656.

Huang J, Wang J, Liu S. 2024. Advances in the production of fungi-derived lignocellulolytic enzymes using agricultural wastes. Mycology. 15(4):523–537. doi: 10.1080/21501203.2023.2253827.

Jones M, Bhat T, Kandare E, Thomas A, Joseph P, Dekiwadia C, Yuen R, John S, Ma J, Wang CH. 2018. Thermal degradation and fire properties of fungal mycelium and mycelium-biomass composite materials. Sci Rep. 8:17583. doi: 10.1038/s41598-018-36032-9.

Kandagalla S, Krishnappa M. 2020. Exploring the ethnomycological potential of *Lentinus squarrosulus* Mont. through GC–MS and chemoinformatics tools. Mycology. 11(1):78. doi: 10.1080/21501203.2019.1707724.

Kohphaisansombat C, Jongpipitaporn Y, Laoratanakul P, Tantipaibulvut S, Euanorasetr J, Rungjindamai N, Boonyuen N. 2024. Fabrication of mycelium (oyster mushroom)-based composites derived from spent coffee grounds with pineapple fibre reinforcement. Mycology. 15(4):665–682. doi: 10.1080/21501203.2023.2273355.

Konara UA, Thambugala KM, Karunarathna SC, Ediriweera A, Hapuarachchi KK. 2024. Unveiling the hidden diversity of *Ganoderma* (Ganodermataceae, Polyporales) in Sri Lanka: the first report of *G. angustisporum*, *G. ellipsoideum*, and *G. orbiforme*. N Z J Botan. 1–25. doi: 10.1080/0028825X.2024.2415555.

Madusanka C, Udayanga D, Nilmini R, Rajapaksha S, Hewawasam C, Manamgoda D, Vasco-Correa J. 2024a. A review of recent advances in fungal mycelium-based composites. Discover Mater. 4(1):13. doi: 10.1007/s43939-024-00084-8.

Madusanka TGC, Udayanga D, Nilmini AHLR, Rajapaksha SM, Hewawasam C, Manamgoda D. 2024b. Development of biodegradable fungal mycelium-based foams from corn husk waste. In: Dissanayake R, Jayasinghe GY, Setunge S, Amaratunga D, Gunawardana L, Gajanayake P, editors. Proceedings of the 1st International Conference on University-Industry Collaborations for Sustainable Development. Singapore: Springer Nature; p. 199–211. doi: 10.1007/978-981-97-5944-6_16.

Majib NM, Yaacob ND, Ting SS, Rohaizad NM, Azizul RAM. 2025. Fungal mycelium-based biofoam composite: a review in growth, properties and application. Prog Rubber Plast Recycl Technol. 41(1):91–123. doi: 10.1177/14777606241252702.

Manamgoda DS, Cai L, McKenzie EH, Crous PW, Madrid H, Chukeatirote E, Shivas RG, Tan YP, Hyde KD. 2012. A phylogenetic and taxonomic re-evaluation of the *Bipolaris-Cochliobolus-Curvularia* complex. Fungal Divers. 56(1):131–144. doi: 10.1007/s13225-012-0189-2.

Miriyagalla SD, Manamgoda DS, Udayanga D. 2022. Molecular characterization and cultivation of edible wild mushrooms, *Lentinus sajor-caju, Lentinus squarrosulus* and *Pleurotus tuber-regium* from Sri Lanka. Curr Res Environm Appl Mycol. 12(1):28–43. doi: 10.5943/cream/12/1/3.

Namphonsane A, Amornsakchai T, Chia CH, Goh KL, Thanawan S, Wongsagonsup R, Smith SM. 2023. Development of biodegradable rigid foams from pineapple field waste. Polymers. 15(13):2895. doi: 10.3390/polym15132895.

Onyeka C, Okwujiako I, Anyado-Nwadike S, Ezeji EU, Ogbulie TE. 2025. *Lentinus squarrosulus* (mont.): successful domestication and regional adaptability in Orlu, Imo State, eastern Nigeria. Curr Res Environ Appl Mycol. 15:22–34. doi: 10.5943/cream/15/1/3.

Prakash V, Kavitha JR, Kamaleshwaran R, Prabharan P, Alagendran S. 2021. Effect of coir pith compost in agriculture. J Med Plants. 9:106–110. doi: 10.22271/plants.

Raj SS, Kuzmin AM, Subramanian K, Sathiamoorthyi S, Kandasamy KT. 2021. Philosophy of selecting ASTM standards for mechanical characterization of polymers and polymer composites. Mater Plast. 58(3):247–256. doi: 10.37358/Mat.Plast.1964.

Robertson O, Høgdal F, McKay L, Lenau T. 2020. Fungal future: A review of mycelium biocomposites as an ecological alternative insulation material. In: Mortensen NH, Hansen CT, Deininger M, editors. DS 101: Proceedings of NordDesign 2020; 12–14 Aug 2020; Lyngby, Denmark: Design Society. p. 1–13. doi: 10.35199/NORDDESIGN2020.18.

Rossi M, Camino G, Luda M. 2001. Characterization of smoke in expanded polystyrene combustion. Polym Degrad Stab. 74 (3):507–512. doi: 10.1016/S0141-3910(01)00168-9.

Saini R, Kaur G, Brar SK. 2024. Textile residue-based mycelium biocomposites from *Pleurotus ostreatus*. Mycology. 15 (4):683–689. doi: 10.1080/21501203.2023.2278308.

Shin HJ, Ro HS, Kawauchi M, Honda Y. 2025. Review on mushroom mycelium-based products and their production process: from upstream to downstream. Bioresour Bioprocess. 12(1):1–21. doi: 10.1186/s40643-024-00836-7.

Sreerag NK, Kashyap P, Shilpa VS, Thakur M, Goksen G. 2025. Recent advances on mycelium based biocomposites: synthesis, strains, lignocellulosic substrates, production parameters. Polym Rev. 65(1):169–198. doi: 10.1080/15583724.2024.2423949.

Sun S, Sun S, Cao X, Sun R. 2019. The role of pretreatment in improving the enzymatic hydrolysis of lignocellulosic materials. Bioresour Technol. 199:49–58. doi: 10.1016/j.biortech.2015.08.061.

Thiribhuvanamala G, Krishnamoorthy AS. 2021. Evaluation of different lignocellulosic substrates for cultivation of medicinal mushroom *Ganoderma lucidum*. J Environ Biol. 42(5):1314–1319. doi: 10.22438/jeb/42/5/MRN-1686.

Vaitkus S, Vėjelis S, Šeputytė-Jucikė J, Członka S, Strzelec K, Kairytė A. 2022. Analysis of active and passive deformation of expanded polystyrene foam under short-term compression. Materials. 15(21):7548. doi: 10.3390/ma15217548.

Vašatko H, Gosch L, Jauk J, Stavric M. 2022. Basic research of material properties of mycelium-based composites. Biomimetics. 7(2):51. doi: 10.3390/biomimetics7020051.

Walker R, Pavia S. 2014. Moisture transfer and thermal properties of hemp–lime concretes. Constr Build Mater. 64:270–276. doi: 10.1016/j.conbuildmat.2014.04.081.

Wei Z, Gu K, Chen B, Wang C. 2023. Comparison of sawdust bio-composites based on magnesium oxysulfate cement and ordinary Portland cement. J Build Eng. 63:e105514. doi: 10.1016/j.jobe.2022.105514.

Whabi V, Yu B, Xu J. 2024. From nature to design: tailoring pure mycelial materials for the needs of tomorrow. J Fungi. 10 (3):183. doi: 10.3390/jof10030183.

Zhou Q, Ou Z, Rao X, Liu Y, Liang C, Zhang L, Huo C, Du X. 2020. Lignin-carbohydrate complexes from coconut (*Cocos nucifera*) coir: fractionation, structural elucidation, and potential applications. BioResources. 15(3):7100–7117. doi: 10.15376/biores.15.3.7100-7117.